

Mechanisms of small clusters production by short and ultra-short laser ablation

Tatiana E. Itina^{a,*}, Karine Gouriet^a, Leonid V. Zhigilei^b, Sylvie Noël^a,
Jörg Hermann^a, Marc Sentis^a

^a *Laboratoire Lasers, Plasmas et Procédés Photoniques (LP3 UMR 6182 CNRS), Faculté des Sciences de Luminy, Case 917, 13288 Marseille, France*

^b *Department of Materials Science & Engineering, University of Virginia, 116 Engineer's Way, Charlottesville, VA 22904-4745, USA*

Available online 20 February 2007

Abstract

The mechanisms involved into the formation of clusters by pulsed laser ablation are studied both numerically and experimentally. To facilitate the model validation by comparison with experimental results, the time and length scales of the simulation are considerably increased. This increase is achieved by using a combination of molecular dynamics (MD) and the direct simulation Monte Carlo (DSMC) methods. The combined MD–DSMC model is then used to compare the relative contribution of the two channels of the cluster production by laser ablation: (i) direct cluster ejection upon the laser-material interaction, and (ii) collisional sticking and aggregation in the ablated gas flow. Calculation results demonstrate that both of these mechanisms play a role. The initial cluster ejection provides cluster precursors thus eliminating the three-body collision bottleneck in the cluster growth process. The presence of clusters thus facilitates the following collisional condensation and evaporation processes. The rates of these processes become considerable, leading to the modification of not only the plume cluster composition, but also the dynamics of the plume expansion. Calculation results explain several recent experimental findings.

© 2007 Elsevier B.V. All rights reserved.

PACS : 52.38Mf; 02.60.Cb

Keywords: Nanoparticles; Laser ablation; Simulation; Clusters

1. Introduction

During the last decade, numerous experiments have been performed, clearly demonstrating that an interaction of a short (several nanoseconds or shorter) laser pulse with a solid target leads to the formation of nanoparticles. This technique, known as pulsed laser ablation (PLA), has become a promising method of the synthesis of nanoclusters for photonics, electronics and medicine [1–12]. The PLA method has several advantages compared to more traditional techniques. In particular, it was shown that this method provides a possibility for chemically clean synthesis, which is difficult to achieve under more conventional nanoparticle production conditions. In addition, several experimental studies indicated that the cluster size distribution could be controlled in PLA by carefully choosing

the laser irradiation parameters and properties of the background gas. Furthermore, laser ablation allows for an easy production of colloidal metal nanoparticles for biological and medical applications.

Despite the large number of the experimental results, the theoretical understanding of the physical and chemical mechanisms leading to the formation of nanoparticles during the PLA is still lacking. The number of theoretical studies of these mechanisms remains limited because both the continuum hydrodynamic models and the classical nucleation theory become inapplicable under the typical PLA conditions. Under these conditions, laser plume expansion and all collisional processes inside the plume occur so rapidly that equilibrium conditions are not attained. In addition, fast laser energy deposition may induce an explosive volume ejection rather than an equilibrium surface evaporation. Nevertheless, the laser ablation process is often described by a thermal desorption model, which considers the ablation as a rather slow layer-by-layer evaporation of monomers from the target surface [13].

* Corresponding author. Tel.: +33 491 82 92 83; fax: +33 491 82 92 89.

E-mail address: itina@lp3.univ-mrs.fr (T.E. Itina).

The presence of nanoparticles in the laser plume is then explained by using a Zeldovich–Raizer condensation model [14–17]. This approach is appropriate for interpretation of the experimental findings obtained in laser ablation with hundred of nanoseconds and longer laser pulses, and in the presence of a background gas [18,19]. In the PLA with shorter laser pulses, however, clusters can be ejected directly from the target as a result of the target disintegration by laser-induced explosion-like process [20–22]. In this case, the common thermal desorption and condensation model is insufficient and only a detailed molecular-level simulation can provide a complete description of the nanoparticle formation process. One of the possible approaches for such simulations is to combine the molecular dynamics technique (MD) with the direct simulation Monte Carlo method (DSMC) [23–28]. This combination allows one to properly account for both the processes of cluster ejection and their following evolution during the laser plume expansion as a result of the gas-phase collisions.

Herein, we present the numerical results obtained with a hybrid MD–DSMC model of PLA for different laser pulses and fluences. The objective of this study is to bridge a gap between the previous molecular dynamics simulations and typical ablation experiments. In fact, the proposed combination of methods allows us to attain both time and length scales typical for ablation experiments. By using the combined model, we investigate the time evolution of clusters in the plume. We examine different types of collisions leading to cluster growth and decay. As a result, we determine the major collisional processes responsible for the observed changes in cluster distributions. These results are related to the recent experimental results on the ablation plume dynamics.

2. Combined MD–DSMC numerical model

2.1. General description of the combined MD–DSMC model

A combined MD–DSMC model is developed for the calculation of the laser plume formation and long-term evolution. In the model, two different numerical methods are used (i) molecular dynamics for target material disintegration and ejection of a mixture of clusters and monomers [22,29] and (ii) direct simulation Monte Carlo for the calculation of large-scale three-dimensional plume evolution [30]. Here, as in the previous MD calculations [22,23,29], the breathing sphere model is adopted to model laser pulse absorption and relaxation processes in the MD part. The calculation parameters in the MD part are the same as in these calculations for a molecular solid target. The pulse duration was set to be 15 ps.

The transition between the DSMC and MD calculations is performed by using the MD results obtained at 1 ns after the laser pulse for the design of the initial conditions for the subsequent DSMC calculation. The collision probabilities in DSMC calculations are parameterized to describe the material properties in a gas phase, such as viscosity coefficient and velocity dependence of the equivalent collision cross sections [31].

2.2. Design of the interface between the MD and DSMC simulations

To couple the two models, all plume species are divided into five groups depending on their size. The groups are chosen as follows: (1) monomers, (2) clusters of 2–15 molecules, (3) clusters of 16–100 molecules, (4) clusters of 101–1000 molecules, and (5) clusters of more than 1000 molecules.

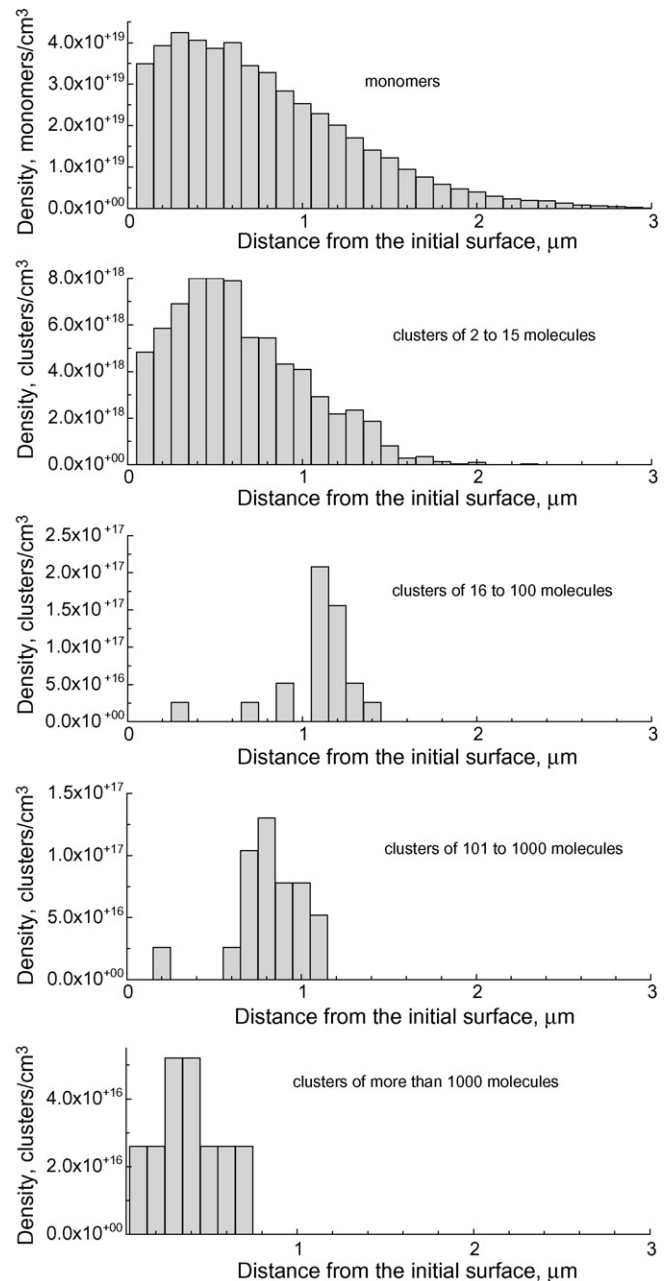


Fig. 1. Number density of clusters of different sizes in the ablation plume as a function of the distance from the initial surface. The data is obtained in a MD simulation of laser ablation of a molecular target performed with a laser pulse width of 15 ps and a fluence of 61 J/m^2 . The results are shown for 1 ns after laser irradiation. The distributions in (b), (c), (d) and (f) are plotted for groups of clusters in order to obtain statistically adequate representations of the spatial distribution of large and medium clusters in the ablation plume.

The results of the molecular dynamics calculations corresponding to these groups are shown in Fig. 1. The calculations are performed with laser pulse duration of 15 ps and an absorbed laser fluence of 61.38 J/m². Cluster size is sampled in each group according to the size distributions obtained in the MD simulation (Fig. 2).

In the present study, we assume that the spatial laser beam profile is top hat and the radial expansion of the ablation plume is small during the first MD stage. Therefore, the radial distributions of the simulation parameters are assumed to be uniform within the laser spot. The axial distributions of the initial DSMC parameters are determined by fitting the axial distributions of density, velocity, radial and axial temperatures for different groups obtained from the MD calculations. To fit the axial density distributions, we use normal distribution functions:

$$f_i(z) = \frac{d_i}{\sigma_i \sqrt{2\pi}} \exp\left[-\frac{(z - \mu_i)^2}{2\sigma_i^2}\right], \quad (1)$$

where z is the distance from the initial target surface. The parameters d_i , μ_i , and σ_i are calculated from numerical fits to the MD results performed for each group, and $i = 1-5$. The linear dependencies:

$$g_i(z) = A_i z - B_i \quad (2)$$

are used to fit axial velocity distributions, where A_i and B_i are fitting parameters for each component [22]. The distributions of the axial and radial temperatures as well as the internal temperatures of the clusters are fitted by six-order polynomial dependencies. More details of the procedure used for the statistical description of the output of MD simulations will be presented elsewhere.

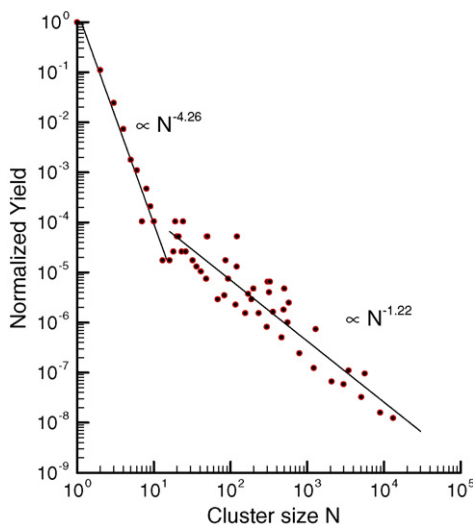


Fig. 2. MD simulation results on cluster abundance distribution in the ablation plume at 1 ns after irradiation with a 15 ps laser pulse at a laser fluence of 61 J/m².

2.3. Modified DSMC method for modeling of ablated flows with clusters and reactions

In the DSMC simulations, the laser plume is modeled by an ensemble of simulated particles (here, about 8×10^6). The simulated particles are introduced based on the gas-dynamic parameters obtained from the MD simulations of the initial stage of the plume formation. The physical space is divided into a network of cells with dimensions smaller than the local mean free path. The time is incremented by a small time step Δt . The calculations consist in the repetition of three main steps: (i) indexing of the simulated particles; (ii) calculation of a representative set of collisions and chemical reactions in each cell; (ii) movement of the simulated particles and calculation of the interactions with the boundaries [24]. In the present work, collisions are calculated for all particles together based on their probabilities by using a NTC technique [24].

The initial and boundary conditions are set as follows. At the beginning, simulated particles are introduced according to the distributions calculated by MD as described in Section 2.2 above. The axis $r = 0$ is set to be the axis of radial symmetry. At the target surface ($Z = 0$), a partial diffuse reflection and re-deposition of particles is sampled by using an accommodation coefficient. The accommodation coefficient of the target surface is set to be 0.5 in this work. The simulated volume is increased several times during the calculation to cover the plume expansion region.

The calculation of collisions and reactions in the present DSMC includes the treatment of the following processes:

- (i) elastic collisions;
- (ii) inelastic non-reactive collisions;
- (iii) sticking reactions in cluster—molecule collisions;
- (iv) aggregation reactions in cluster—cluster collisions;
- (v) cluster evaporation reactions.

The non-reactive collisions are calculated based on the conservation laws of energy and momentum. For clusters, the reference cross-sections are computed based on their effective radii [31] $r_n = an^{1/3} + b$, where $a = 3.97 \text{ \AA}$, $b = 1.59 \text{ \AA}$, n is the number of monomers in the cluster. A soft-spheres collision model is used in the present modeling calculation. As we described above, the initial values of the internal energy, E_n , are assigned to each cluster based on the internal temperature distribution obtained from the MD simulation and the number of degree freedom in the cluster. To describe the internal energy modification in clusters and small molecules, Larsen–Borgnakke statistical model [24] is used. Sticking process is included for collisions in which the relative translational energy before the collision is smaller than the binding energy of the final cluster. In this case, the sticking of two clusters containing n_1 and n_2 molecules occurs with the probability [32]:

$$p_1 = p_0 \times (n_1 n_2)^{-x}, \quad (3)$$

where x is a parameter ($x = 1/12$ in the present simulation [32]), and p_0 is a constant. The parameters in (3) are selected based on

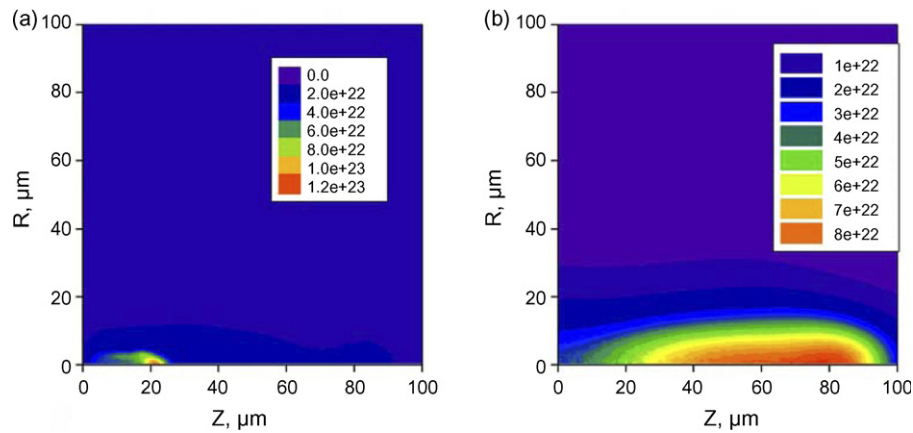


Fig. 3. Two-dimensional distributions of (a) cluster number density and (b) monomer density at a time delay of 50 ns. The results are obtained in a MD–DSMC simulation performed for a pulse duration of 15 ps, laser fluence of 61 J/m^2 , and a laser spot radius of $10 \text{ }\mu\text{m}$.

a separate MD study of cluster evolution in a gas (to be published in a forthcoming paper). The binding energy in each cluster is given by a combination of volume and surface terms:

$$E_b = a_v n - a_s n^{2/3}, \quad (4)$$

where a_v and a_s are material constants and n is the number of molecules in the cluster. To ensure the energy conservation in the sticking reaction, the relative translational energy of the monomer and cluster was transferred into the internal energy of the resulting cluster, whereas the center-of-mass velocity was conserved.

The rate of evaporation from a cluster of n atoms with internal energy E_n is calculated according to the RRK theory [33,34] with the following rate coefficient

$$k_{ev} = C \left[\frac{E_n - D_n}{E_n} \right]^{v_n - 1}, \quad (5)$$

where E_n is the cluster internal energy, $C = \alpha \nu g_n$, α is a constant, $\nu = 10^{13} \text{ s}^{-1}$ the atomic vibration frequency in the cluster, v_n the number of vibrational degrees of freedom; $g_n = (36\pi)^{1/3} (n^{1/3} - 1)^2$ is the number of surface molecules. For clusters containing five molecules or less, the evaporation energy was set to be constant, $D_n = 0.6 \text{ eV}$. For larger clusters, the evaporation energy is [35]:

$$D_n = E_{bn} - E_{b(n-1)} = a_v - a_s [n^{2/3} - (n-1)^{2/3}] \quad (6)$$

where $a_v = 0.6$ and $a_s = 0.73 \text{ eV}$ in our simulation performed for a molecular target. After the evaporation, the internal energy of the remaining cluster is decreased. The energy difference goes into the relative translational energy of the evaporated monomer and the parent cluster and in the internal energy of the monomer.

3. Results and discussion

A series of calculations are performed with the combined MD–DSMC model. First, we consider the laser plume dynamics. Distributions of the cluster and monomer densities shown in Fig. 3 illustrate the laser plume expansion away from

the irradiated target. Monomers constitute the fastest plume component, whereas clusters are moving slower. In addition, we find that the larger are clusters the lower is their average axial velocity. Quantitatively, the center-of-mass velocity of the monomer component of the plume is about 1560 m/s , whereas

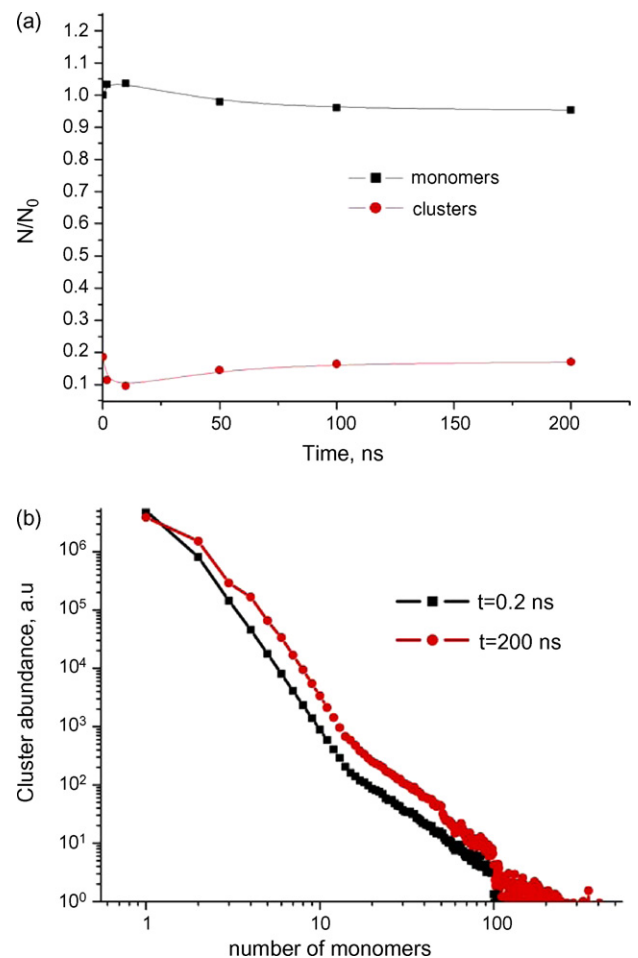


Fig. 4. (a) Time evolution of the number of monomers and clusters in the plume. (b) Cluster abundance distribution. The results are obtained in a MD–DSMC simulation performed for a pulse duration of 15 ps, laser fluence of 61 J/m^2 and a laser spot radius of $10 \text{ }\mu\text{m}$.

the one of clusters is as small as 555 m/s. Here, clusters bigger than 10 molecules were considered.

Furthermore, the changes in the plume composition and the influence of evaporation/condensation processes are examined. In order to provide a reliable description of the evaporation/condensation processes in DSMC, the cluster evolution is first investigated in a separate 5 ns long MD simulation performed for a gas box containing one cluster of a given initial size and temperature. These calculations demonstrate that, for temperatures observed by the end of MD simulations of laser ablation, small cluster evaporation prevailed over growth within the considered time of 5 ns. The parameters used in the DSMC part are adjusted to these results.

The evolution of the plume composition in the MD-DSMC simulation of plume expansion is shown in Fig. 4(a). One can see that at the beginning and until about 10 ns, the number of clusters decreases, whereas the number of monomers rises. After that, the situation changes and the number of clusters in the plume steadily increases. At a delay of 200 ns, the number of clusters reaches the one that was in the plume at 1 ns after the

beginning of laser pulse. If one looks at the cluster abundance distribution (Fig. 4(b)), which also varies with time, one can see that the number of small clusters decreases, while bigger clusters become more abundant.

As we have already seen from the MD calculations, the cluster size distribution obtained soon after the ejection is a decaying function. During the following plume expansion, numerous collisions take place in the plume and affect the distribution. The indication of these changes obtained in the MD-DSMC is displayed in Fig. 4(b). One can see the decrease in the number of small clusters and the growth in the number of average ones. The distribution shape agrees with the experimental findings. These results will be discussed in more details elsewhere.

The calculations may help explaining the results of the experiments on plume imaging and spectroscopy obtained for short and ultra-short laser pulses. Fig. 5 shows typical plume images recorded in our laboratory at different times in ultra-short laser ablation experiments with pulse width of 100 fs at 400 nm wavelength. One can clearly observe two different plumes: the faster one and the slower one. Based on our simulation results and on additional spectroscopic study, we can conclude that the first component is composed of atoms and small clusters and the slower one is composed of bigger clusters. More details about the experimental results will be presented elsewhere [36].

4. Summary

To summarize, both the calculations performed with the combined MD-DSMC model and the experiments clearly demonstrate the role of two following channels of the cluster production by short-pulsed laser ablation:

- (i) direct cluster ejection upon the laser-material interaction;
- (ii) collision-affected condensation and evaporation in the ablated plume flow.

The first process results from the fast energy absorption by the target, which leads to the explosive decomposition of a substantial volume of the rapidly heated target material. For short laser pulses, material decomposition might occur through either “phase-explosion” [9,22,23,26,37], photomechanical spallation [23,29,38], or fragmentation [21,39,40] mechanisms. These processes take place in volume rather than on the surface and lead to the ejection of a mixture of clusters and monomers.

The second mechanism is due to gas-phase collisions and evaporations. These processes are similar to the phenomena taking places in aggregation sources [28,41]. The major advantage of short and ultra-short laser pulses for cluster synthesis is the presence of the laser-ejected small molecules and clusters in the ablated flow. As a result, the formation of diatomic molecules in three-body collisions, which represents a “bottleneck” for cluster formation in common aggregation sources, is not crucial for cluster synthesis by short laser ablation.

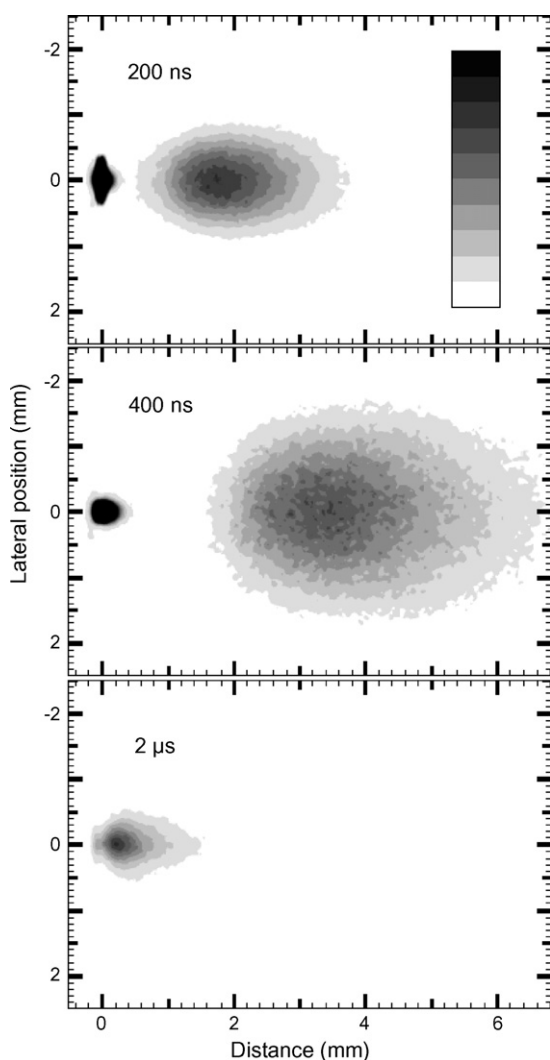


Fig. 5. Plume images recorded at different times in ultra-short laser ablation experiments with Cu. Here, pulse duration is 100 fs and laser fluence is 4 J/cm².

In addition, the MD calculations demonstrate that clusters are segregated in the plume, with larger clusters moving slower and located closer to the target. As a result, during the further expansion of a multiple-component plume, modelled in the DSMC simulations, the segregation of clusters in the plume becomes more pronounced, leading to the formation a complex multi-component plume structure. These results agree with recent experimental studies of ultra-short laser pulse ablation, where continuous emission was observed from the delayed plume component.

Acknowledgments

We gratefully acknowledge financial support provided by the National Science Foundation (NSF) and the Centre National de la Recherche Scientifique (CNRS) through a US-France Cooperative Research grant. LVZ also acknowledges additional support from the NSF (CTS-0348503). We are thankful to the IDRIS and the CINES of CNRS, France for the computer support.

References

- [1] I. Movtchan, R.W. Dreyfus, W. Marine, M. Sentis, M. Autric, G. Le Lay, *Thin Solid Films* 286 (1995) 255.
- [2] Y. Yamada, T. Orii, I. Umezumi, S. Takeyama, Y. Yoshida, *Jpn. J. Appl. Phys. Part 1* 35 (1996) 1361.
- [3] T. Makimura, Y. Kunii, K. Murakami, *Jpn. J. Appl. Phys. Part 1* 35 (1996) 4780.
- [4] T. Makimura, T. Mizuta, K. Murakami, *Appl. Phys. Lett.* 76 (2000) 1401.
- [5] I.A. Movtchan, W. Marine, R.W. Dreyfus, H.C. Le, M. Sentis, M. Autric, *Appl. Surf. Sci.* 251 (1996) 96–98.
- [6] D.B. Geohegan, A.A. Puretzky, G. Dusher, S.J. Pennycook, *Appl. Phys. Lett.* 72 (1998) 2987.
- [7] L. Patrone, D. Nelson, V.I. Safarov, M. Sentis, W. Marine, S. Giorgio, *J. Appl. Phys.* 87 (2000) 3829.
- [8] W. Marine, L. Patrone, B. Luk'yanchuk, M. Sentis, *Appl. Surf. Sci.* 345 (2000) 154–155.
- [9] I. Ozerov, D. Nelson, A. Bulgakov, W. Marine, M. Sentis, *Appl. Surf. Sci.* 349 (2003) 212–213.
- [10] A.V. Kabashin, M. Meunier, *J. Appl. Phys.* 94 (2003) 7901.
- [11] O. Albert, S. Roger, Y. Glinec, J.C. Loulergue, J. Etchepare, C. Boulmer-Leborgne, J. Perriere, E. Millon, *Appl. Phys. A: Mater. Sci. Process.* 76 (2003) 319.
- [12] D. Scuderi, R. Benzerga, O. Albert, B. Reynier, J. Etchepare, *Appl. Surf. Sci.* 252 (13) (2006) 4360–4363.
- [13] S.I. Anisimov, *Zh. Eksp. Teor. Fiz.* 54 (1968) 339 [*Sov. Phys. JETP* 27 182 (1968)].
- [14] Y.B. Zeldovich, Y.P. Raizer, *Physics of Shock Waves and High Temperature Hydrodynamic Phenomena*, Academic Press, London, 1966.
- [15] B. Luk'yanchuk, W. Marine, S. Anisimov, *Laser Phys.* 8 (1998) 291.
- [16] B.S. Luk'yanchuk, W. Marine, S.I. Anisimov, G.A. Simakina, *Proc. SPIE* 3618 (1999) 434–452.
- [17] A.V. Gusarov, A.V. Gnedovets, I. Smurov, *J. Appl. Phys.* 88 (2000) 4362.
- [18] T. Ohkubo, M. Kuwata, B. Luk'yanchuk, T. Yabe, *Appl. Phys. A* 77 (2003) 271.
- [19] A.S. Boldarev, V.A. Gasilov, F. Blasco, C. Stenz, F. Dorchies, F. Salin, A.Y. Faenov, T.A. Pikuz, A.I. Magunov, I. Yu Skobelev, *JETP Lett.* 73 (2001) 514.
- [20] A.V. Bulgakov, I. Ozerov, W. Marine, *Appl. Phys. A* 79 (2004) 1591.
- [21] S. Amoroso, R. Bruzzese, N. Spinelli, R. Velotta, M. Vitello, X. Wang, *Europhys. Lett.* 67 (2004) 404.
- [22] L.V. Zhigilei, *Appl. Phys. A* 76 (2003) 339.
- [23] L.V. Zhigilei, B.J. Garrison, *J. Appl. Phys.* 88 (3) (2000) 1281.
- [24] G.A. Bird, *Molecular Gas Dynamics and the Direct Simulation of Gas Flows*, Clarendon, Oxford, 1994.
- [25] T.E. Itina, J. Hermann, P. Delaporte, M. Sentis, *Phys. Rev. E* 66 (2002) 066406.
- [26] M.I. Zeifman, B.J. Garrison, L.V. Zhigilei, *J. Appl. Phys.* 92 (2002) 2181.
- [27] H. Mizuseki, Y. Jin, Y. Kawazoe, L.T. Wille, *Appl. Phys. A* 73 (2001) 731.
- [28] B. Briehl, H.M. Urbassek, *J. Vac. Sci. Technol. A* 17 (1999) 256.
- [29] L.V. Zhigilei, B.J. Garrison, *J. Appl. Phys.* 88 (2000) 1281.
- [30] T.E. Itina, V.N. Tokarev, W. Marine, M. Autric, *J. Chem. Phys.* 106 (1997) 8905.
- [31] M.I. Zeifman, B.J. Garrison, L.V. Zhigilei, *AIAA Paper* 2003, 2003.
- [32] H. Hittema, J.S. McFeaters, *J. Chem. Phys.* 105 (1996) 2816.
- [33] J.W. Brady, J.D. Doll, D.L. Thompson, *J. Chem. Phys.* 71 (1979) 2467.
- [34] M.F. Jarold, in: H. Haberland (Ed.), *Clusters of Atoms and Molecules*, Springer, Berlin, 1994, p. 163.
- [35] A. Malakhovskii, M. Ben-Zion, *Chem. Phys.* 264 (2001) 135.
- [36] S. Noël, J. Hermann and T. Itina, *Appl. Surf. Sci.* In Press, Available online 30 January 2007.
- [37] B.J. Garrison, T.E. Itina, L.V. Zhigilei, *Phys. Rev. E* 68 (2003) 041501.
- [38] E. Leveugle, D.S. Ivanov, L.V. Zhigilei, *Appl. Phys. A* 79 (2004) 1643.
- [39] D. Perez, L.J. Lewis, *Phys. Rev. Lett.* 89 (2002) 25504.
- [40] T.E. Glover, *J. Opt. Soc. Am. B* 20 (2003) 125.
- [41] H. Haberland, in: H. Haberland (Ed.), *Clusters of Atoms and Molecules*, Springer, Berlin, 1994, p. 205.